AJNR

MR Imaging Detection of Cerebral Microbleeds: Effect of Susceptibility-Weighted Imaging, Section Thickness, and Field Strength

R.N.K. Nandigam, A. Viswanathan, P. Delgado, M.E. Skehan, E.E. Smith, J. Rosand, S.M. Greenberg and B.C. Dickerson

AJNR Am J Neuroradiol 2009, 30 (2) 338-343
doi: https://doi.org/10.3174/ajnr.A1355
http://www.ajnr.org/content/30/2/338

ORIGINAL RESEARCH

MR Imaging Detection of Cerebral Microbleeds: Effect of Susceptibility-Weighted Imaging, Section Thickness, and Field Strength

R.N.K. Nandigam
A. Viswanathan
P. Delgado
M.E. Skehan
E.E. Smith
J. Rosand
S.M. Greenberg
B.C. Dickerson

BACKGROUND AND PURPOSE: The emergence of cerebral microbleeds (CMB) as common MR imaging findings raises the question of how MR imaging parameters influence CMB detection. To evaluate the effects of modified gradient recalled-echo (GRE) MR imaging methods, we performed an analysis of sequence, section thickness, and field strength on CMB imaging properties and detection in subjects with cerebral amyloid angiopathy (CAA), a condition associated with microhemorrhage.

MATERIALS AND METHODS: Multiple MR images were obtained from subjects with probable CAA, with varying sequences (GRE versus susceptibility-weighted imaging [SWI]), section thicknesses (1.2–1.5 versus 5 mm), and magnetic field strengths (1.5T versus 3T). Individual CMB were manually identified and analyzed for contrast index (lesion intensity normalized to normal-appearing white matter signal intensity) and diameter. CMB counts were compared between 1.5T thick-section GRE and thin-section SWI for 3 subjects who underwent both protocols in the same scanning session.

RESULTS: With other parameters constant, use of SWI, thinner sections, and a higher field strength yielded medium-to-large gains in CMB contrast index (CI; Cohen d 0.71–1.87). SWI was also associated with small increases in CMB diameter (Cohen d <0.3). Conventional thick-section GRE identified only 33% of CMB (103 of 310) seen on thin-section SWI. Lesions prospectively identified on GRE had significantly greater CI and diameter measured on the GRE image than those not prospectively identified.

CONCLUSIONS: The examined alternatives to conventional GRE MR imaging yield substantially improved CMB contrast and sensitivity for detection. Future studies based on these techniques will most likely yield even higher prevalence estimates for CMB.

Advances in MR imaging technology have led to improved sensitivity to deposited hemosiderin, which has facilitated the recognition that cerebral microbleeds (CMB) are a relatively common neuroimaging finding.[1-6] These lesions, composed pathologically of clusters of hemosiderin-containing macrophages, which are often perivascular,[7,8] appear as round hypointense foci on gradient recalled-echo (GRE) MR imaging sequences weighted for magnetic susceptibility effects. They are particularly prevalent in association with hemorrhagic stroke due to cerebral amyloid angiopathy (CAA)[9] or hypertensive vasculopathy[10,11] but can also be seen with ischemic stroke,[12] Alzheimer disease,[13,14] cerebral autosomal dominant arteriopathy with subcortical infarctions and leukoencephalopathy,[15] or normal aging.[5,6] CMB have been suggested as potential markers of a hemorrhage-prone state[12,16,17] or of vascular cognitive impairment.[18]

As it has become clear that our understanding of CMB is heavily dependent on MR imaging methodology,[4] several potential techniques to enhance the sensitivity of MR imaging of CMB have emerged. These include the recently developed technique of susceptibility-weighted imaging (SWI),[19] the use of higher resolution to decrease partial volume averaging of CMB with surrounding brain tissue,[20] and the use of higher magnetic field strengths to improve the source of contrast and signal-intensity-to-noise ratio.[21,22] Enhanced MR imaging sensitivity could potentially increase the measured prevalence of CMB. For example, a recent report from the population-based Rotterdam Scan Study,[6] by using an optimized sequence of high resolution and long TEs, found a surprisingly high prevalence of CMB (ranging from 17.8% of individuals 60–69 years of age to 38.3% for those ≥80).

Although the detection of CMB is heavily influenced by a variety of MR imaging parameters, there has been relatively little investigation of the specific effects of these parameters on CMB detection. We, therefore, undertook a systematic comparison of MR imaging scanning parameters in subjects known to have multiple corticosubcortical CMB diagnosed as due to CAA. Specifically, we sought the following: 1) to investigate the effects of sequence (traditional GRE versus SWI), section thickness (conventional 5-mm versus thin 1.2- to 1.5-mm sections), and field strength (1.5T versus 3T) on CMB imaging properties such as contrast and diameter; 2) to determine how these imaging properties affect the ability of a rater to identify particular lesions; and 3) to determine the overall effect of more sensitive MR imaging techniques on the number of detected CMB.

Materials and Methods

Research Subjects

Study subjects were recruited from an ongoing single-center prospective longitudinal cohort study of CAA.[23,24] Subjects were patients

Received August 5, 2008; accepted after revision September 9.

From the Hemorrhagic Stroke Research Program (R.N.K.N., A.V., P.D., M.E.S., E.E.S., J.R., S.M.G.) and Alzheimer's Disease Research Center (B.C.D.), Department of Neurology, Massachusetts General Hospital and Harvard Medical School, Boston, Mass; and Athinoula A. Martinos Center for Biomedical Imaging (B.C.D.), Charlestown, Mass.

This work was supported by National Institutes of Health Grants (R01 AG026484, K24 NS056207, R01 AG029411).

Paper previously presented in part at: Annual Meeting of the American Academy of Neurology, April 12-19, 2008; Chicago, Ill.

Please address correspondence to: Steven M. Greenberg, MD, PhD, Massachusetts General Hospital Stroke Research Center, 55 Fruit St, CPZ 175, Ste 300, Boston, MA 02114; e-mail: sgreenberg@partners.org

DOI 10.3174/ajnr.A1355

Table 1: MR imaging acquisition parameters

Sequence	GRE	GRE	SWI	SWI	GRE	SWI
Field strength (Tesla)	1.5	1.5	1.5	1.5	3.0	3.0
Section thickness (mm)	5	1.5	5	1.3	5	1.2
Gap between sections (mm)	1	0.3	0	0	0	0
In-plane resolution (mm)	0.9 × 0.9	0.7 × 0.7	0.9 × 0.9	0.7 × 0.7	1.15 × 1.15	0.5 × 0.5
Acquisition time (min)	3.5	11	2.5	8.5	2.5	9
TR (ms)	750	763	48	48	750	27
TE (ms)	24	24	40	40	25	21
Flip angle (degrees)	30	30	20	20	15	15
Number of averages	2	2	1	1	2	1
Acquisition matrix	256 × 144	320 × 216	256 × 171	320 × 214	192 × 192	448 × 299
FOV (mm)	230 × 130	224 × 151	230 × 130	224 × 150	221 × 221	224 × 150

Note:—GRE indicates gradient recalled-echo; SWI, susceptibility-weighted imaging.

≥55 years of age who presented to the Massachusetts General Hospital between August 2001 and August 2005 with symptomatic lobar intracerebral hemorrhage and met the Boston Criteria for probable CAA based on clinical evaluation and imaging showing multiple hemorrhages restricted to corticosubcortical brain regions.[25] Fourteen subjects with probable CAA each underwent between 2 and 5 (median, 3 per subject) of the 6 MR imaging sequences examined in the current study (Table 1). All study procedures were approved by the Human Research Committee of our institution and were performed after obtaining informed consent.

MR Imaging

Study subjects underwent MR imaging examinations with variations of sequence (conventional GRE versus SWI), section thickness (5 versus 1.2–1.5 mm), and magnetic field strength (1.5T Avanto versus 3T Trio by using a 12-channel Total Imaging Matrix head coil; both Siemens Medical Systems, Erlangan, Germany). Imaging parameters for all sequences are shown in Table 1. SWI processing was performed by Siemens product software incorporated into the MR imaging system console according to published methods.[26]

Analysis of CMB

Image data were first visually inspected by a trained operator (R.N.K.N.). Round hypointense lesions were identified as CMB as described by Greenberg et al.[9,16] As in our previous reports, hypointense lesions were excluded if they appeared to be vascular flow voids (based on sulcal location or linear shape), basal ganglia mineralization, artifact from adjacent bone or sinus, or part of a larger macrohemorrhagic lesion.

To determine the signal-intensity characteristics of CMB on different MR pulse sequences, individual lesions on different images from the same patient were identified by comparison of the images, by using local anatomic landmarks for reference. Individual lesions were then labeled for paired analyses, by using Display Imaging software (Version 1.4.1; McConnell Brain Imaging Center, Montreal Neurologic Institute, Montreal, Canada). Two parameters were measured for each CMB: contrast index (CI) and diameter. To determine CI, we measured the mean signal intensity (SI) in a region of interest placed over the CMB in a single section (magnified to facilitate region-of-interest placement) and in a region of interest of similar size placed on a single section of normal-appearing white matter of the corpus callosum. CI was defined by the following formula: $CI = (SI_{WM} - SI_{CMB}) / SI_{WM}$, where SI_{CMB} is the mean signal intensity of the CMB region of interest and SI_{WM} is the mean signal intensity of the corpus callosum white matter. CMB diameter was obtained by first measuring the cross-sectional area of the CMB region of interest. CMB diameter (D_{CMB}) was then calculated on the basis of the assumption that the region visible on a single section represents a circular cross-section of a spherical lesion, by using the formula $D_{CMB} = 2\sqrt{(A/\pi)}$, where A is the cross-sectional area of the CMB region of interest in square millimeters.

To compare the overall sensitivity for CMB detection between the commonly used clinical GRE sequence (1.5T, 5-mm section thickness) and thin-section SWI (1.5T, 1.3-mm section thickness), a single rater (A.V.) counted CMB on scans of subjects with probable CAA who underwent both studies. All scans of a single-sequence type were presented to the rater in a random order and in a blinded fashion. The SWI and GRE images were analyzed approximately 3 weeks apart to minimize the influence of the prior analysis. With the labels placed on individual CMB on a subject's clinical GRE and thin-section SWI images, the CMB that were identifiable on both scans could be classified according to whether they were prospectively identified by the blinded rater on the GRE as well as the SWI images, or whether they were prospectively identified by the blinded rater solely on the SWI image and identified on the GRE images only in retrospect through comparison with SWI. These 2 classes of CMB were compared for their CI and diameter measured on the GRE image to determine the effect of these lesion properties on whether a CMB could be prospectively identified.

We ascertained intrarater reliability for determination of CI and diameter on 20 randomly selected microbleeds analyzed by a single rater (R.N.K.N.). The 20 CMB were presented to the rater in a random order >2 months after their initial analysis. We also analyzed inter-rater reliability for the number of CMB on thin-section SWI 1.5T images by having 2 raters (A.V. and P.D.) count CMB on images from 8 subjects. Intra- and inter-rater reliability was quantified by the intraclass correlation coefficient (ICC). We have previously demonstrated high inter-rater reliability for CMB counted on clinical GRE images (ICC = 0.97).[9]

Statistical Analysis

CI and diameter of individual CMB seen on multiple sequences were compared by using paired *t* tests. Effect size for the difference between CI and diameter of individual lesions was determined by Cohen d,[27] calculated as the difference of the means divided by the pooled SD. An effect size $d \leq 0.5$ is generally interpreted as a small effect; between 0.5 and 0.8, as a medium effect; and ≥0.8, as a large effect.[27]

Results

Fourteen patients (mean age, 73.4 ± 8.4 years; range, 55–86 years) diagnosed with probable CAA underwent from 2 to 5 of the 6 investigated MR imaging protocols (Table 1), with sys-

Table 2: Effect of sequence parameters, section thickness, and field strength on CI and diameter of microbleeds

Comparator Parameters	No. of CMB (No. of subjects)	Mean ± SD		*P* Value	Cohen D
GRE vs SWI					
At 1.5T thin-section	170 (5)	GRE	SWI		
CI		0.40 ± .16	0.65 ± .10	<.0001	1.87
Diameter (mm)		2.51 ± .87	2.76 ± .94	<.0001	0.28
At 1.5T thick-section	79 (3)	GRE	SWI		
CI		0.25 ± .15	0.49 ± .14	<.0001	1.65
Diameter (mm)		3.03 ± 1.32	3.35 ± 1.69	.0004	0.21
Thick vs Thin Sections					
At 1.5T GRE	138 (5)	Thick section	Thin section		
CI		0.20 ± .14	0.40 ± .15	<.0001	1.38
Diameter (mm)		3.07 ± 1.76	2.51 ± 0.85	<.0001	0.41
At 1.5T SWI	79 (2)	Thick section	Thin section		
CI		0.49 ± .18	0.67 ± .10	<.0001	1.24
Diameter (mm)		3.21 ± 1.76	2.94 ± 1.28	.0037	0.18
1.5T vs 3T					
At thick-section GRE	119 (4)	1.5T	3T		
CI		0.23 ± .14	0.34 ± .17	<.0001	0.71
Diameter (mm)		3.09 ± 1.41	3.45 ± 1.50	<.0001	0.25
At thin-section SWI	29 (1)	1.5T	3T		
CI		0.67 ± .07	0.73 ± .06	.0001	0.88
Diameter (mm)		2.50 ± 0.66	2.26 ± 0.55	.0001	0.40

Note:—CI indicates contrast index; CMB, cerebral microbleeds.

tematic variations in sequence (GRE versus SWI), section thickness (1.2–1.5 versus 5 mm), and magnetic field strength (1.5T versus 3T). Quantitative analysis was performed within the same subject across multiple scan types to investigate the influence of these MR imaging data-acquisition parameters on CMB characteristics, in particular lesion contrast, measured as a CI of signal intensity of the CMB relative to normal-appearing white matter, and lesion diameter. Analysis of 20 randomly selected CMB scored on 2 separate occasions demonstrated reasonably high intrarater reliability for both parameters (ICC = 0.90 for CI measurement, ICC = 0.80 for diameter measurement).

Effect of Sequence, Section Thickness, and Magnetic Field Strength on CMB Characteristics

Comparisons of CI and diameter for each CMB that could be identified on 2 separate MR imaging protocols are shown in Table 2. SWI compared with GRE was associated with a large increase in CMB CI (Cohen d >1.5) and a small increase in CMB diameter (Cohen d <0.3) when performed at 1.5T with either thin or thick sections. Thin MR imaging sections, compared with thicker sections, were associated with a large increase in CMB CI (Cohen d >1.2) and a small decrease in CMB diameter (Cohen d <0.5) when performed at 1.5T by using either GRE or SWI parameters. Higher magnetic field strength, compared with lower magnetic field strength, was associated with a moderate-to-large increase in CMB CI (Cohen d 0.7–0.9) when performed with either thick-section GRE or thin-section SWI parameters. Higher magnetic field strength was also associated with a small increase in CMB diameter on thick-section GRE and a small decrease in diameter on thin-section SWI (both Cohen d ≤0.4). Examples of improved lesion contrast associated with SWI, thin MR imaging sections, and 3T field strength are shown in Fig 1.

Effect of MR Imaging Parameters and CMB Characteristics on Visual Identification of CMB

To assess the overall effect of thin-section SWI imaging on identification of CMB, we compared CMB detection on thin-section (1.3 mm) 1.5T SWI images with detection on conventional thick-section (5 mm) 1.5T GRE images obtained in the same scanning session. On the basis of counting of CMB on the SWI images by a second rater (P.D.), we found inter-rater reliability for CMB counts by this method to be high (ICC = 0.93). In 3 subjects who underwent both scanning protocols in a single session, the conventional GRE identified only 33% of CMB (103 of 310) seen on thin-section SWI (Table 3). All but 4 of the additional CMB detected by thin-section SWI were in corticosubcortical or lobar brain regions; the remaining 4 lesions were in the basal ganglia or thalamus.

We next investigated the quantitative measures of CMB CI and diameter to determine if these lesion characteristics influenced whether a CMB was prospectively counted as a lesion. We identified 65 individual CMB on the GRE images from 2 subjects who underwent both conventional 1.5T GRE and thin-section 1.5T SWI and classified them by whether they were prospectively identified on the GRE image alone (21 of the 65) versus whether they were identified on the GRE images only by retrospective comparison with the SWI image (44 of 65). The CI was substantially higher for CMB identified on GRE alone relative to those that were identified retrospectively (0.36 ± 0.11 versus 0.16 ± 0.17, $P < .001$; Fig 2*A*). Lesions counted on GRE alone were also significantly larger, with a mean diameter of 2.4 ± 0.7 mm versus 2.0 ± 0.6 mm ($P = .022$; Fig 2*B*). As seen in Fig 2*C*, most counted CMB had a CI greater than 0.30. However, even some CMB with lower CIs could be identified on GRE if their diameters were relatively large (Fig 2*C*, *solid arrow*), whereas some CMB with CI well above 0.30 were not counted if their diameters were small (*dashed arrow*).

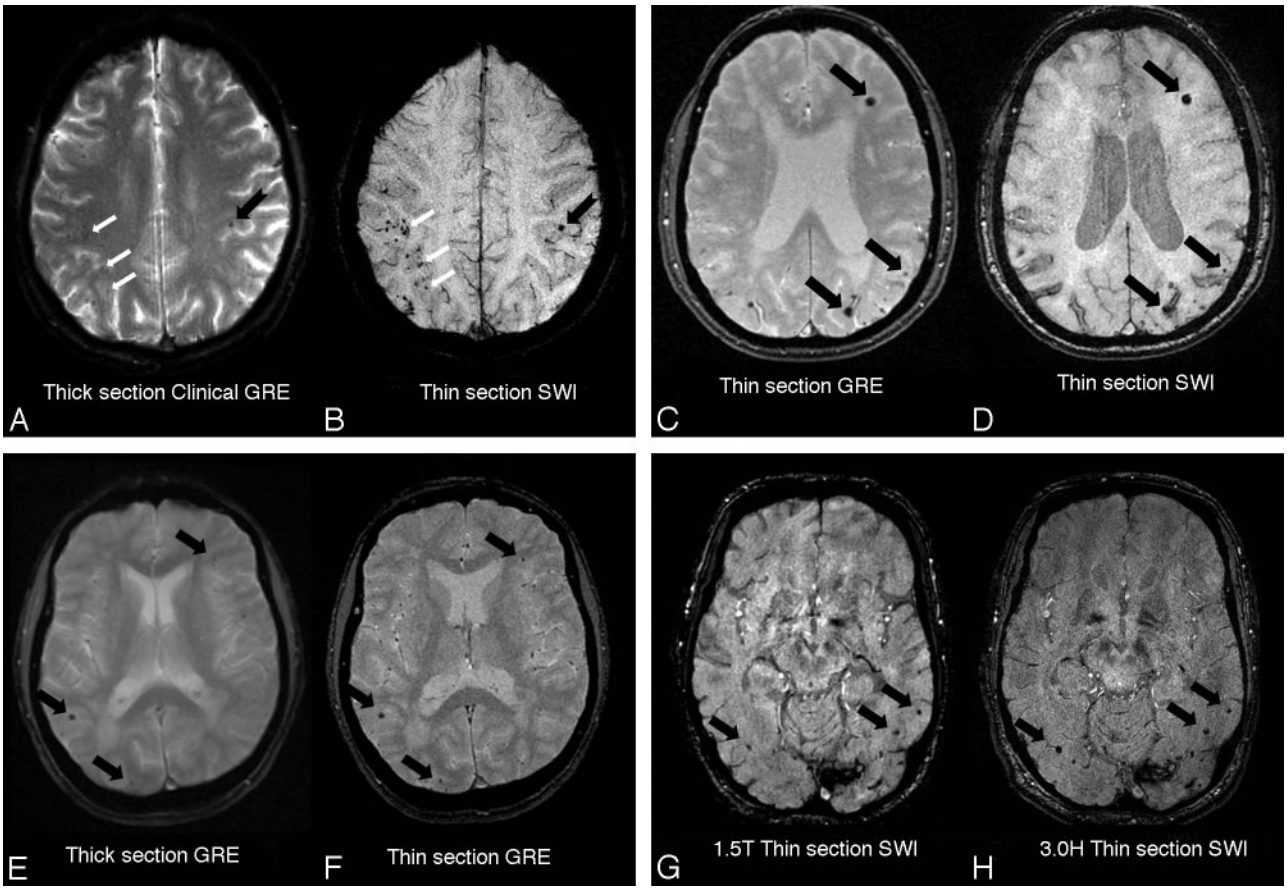

Fig 1. MR images from individual subjects illustrating increased contrast. The pairs of images illustrate comparisons of thick-section GRE (*A*) versus thin-section SWI (*B*, Table 3); thin-section GRE (*C*) versus thin-section SWI (*D*); thick-section GRE (*E*) versus thin-section GRE (*F*; all preceding images at 1.5T); and SWI at 1.5T (*G*) versus SWI at 3T (*H*). Image parameters are shown in Table 1. The black arrows in Fig 2*A* and *B* illustrate a CMB prospectively counted on both sequences, whereas lesions denoted by white arrows were initially identified only on the SWI image. The black arrows in the remaining images highlight lesions on the paired images for comparison.

Table 3: Blinded counting of total number of microbleeds on concurrent clinical GRE and thin-section SWI of individual subjects

Subject No.	Clinical GRE (5-mm sections)	SWI, Thin Section (1.3-mm sections)	% CMB Identified on GRE
1	59	174	34
2	22	84	26
3	22	52	42
Total	103	310	33

Discussion

The major findings from this analysis were the following: 1) SWI, smaller section thickness, and higher magnetic field each yielded substantially increased lesion contrast for CMB, 2) identification of CMB by a trained rater was determined by lesion contrast and (to a lesser extent) diameter, and 3) the overall number of CMB detected depended markedly on the MR imaging technique, with thin-section SWI MR imaging demonstrating approximately 3 times as many lesions as conventional GRE MR imaging in concurrently imaged patients with CAA. SWI was also associated with a small increase in CMB diameter, whereas thin-section imaging yielded slightly decreased lesion diameter.

The additional CMB detected by thin-section SWI in these CAA subjects were almost exclusively (>98%) located in the same lobar brain regions as those detected by conventional GRE. Hemorrhages associated with CAA (both symptomatic macrobleeds and asymptomatic CMB) are characteristically located in these lobar regions.[25] The current findings, therefore, suggest that the additional lesions identified by thin-section SWI are indeed CAA-related CMB rather than some type of non-CMB artifact. This is a reassuring observation given the a priori concern that highly sensitive MR imaging techniques might detect non-CMB lesions, potentially lowering their specificity for CMB.

Because the basis for the MR imaging contrast of these small hemosiderin-laden lesions is susceptibility-related signal-intensity loss due to their ferromagnetic composition, it is not surprising that a sequence designed to be sensitive to these signal-intensity properties (SWI) and a higher field strength (susceptibility effects scale increasingly with field strength) would increase their detection. Furthermore, partial voluming effects (reduction of specific signal intensity caused by combination with signal intensity from nearby tissue with different magnetic properties) are smaller at higher resolution; thus, as long as the signal-intensity-to-noise ratio is maintained, it is reasonable to predict that small lesions such as CMB would be better detected with higher resolution parameters. The major trade-off for both SWI and higher resolution GRE is longer scanning-acquisition time, which may be an issue of concern in patients who have difficulty remaining motionless in the scanner.

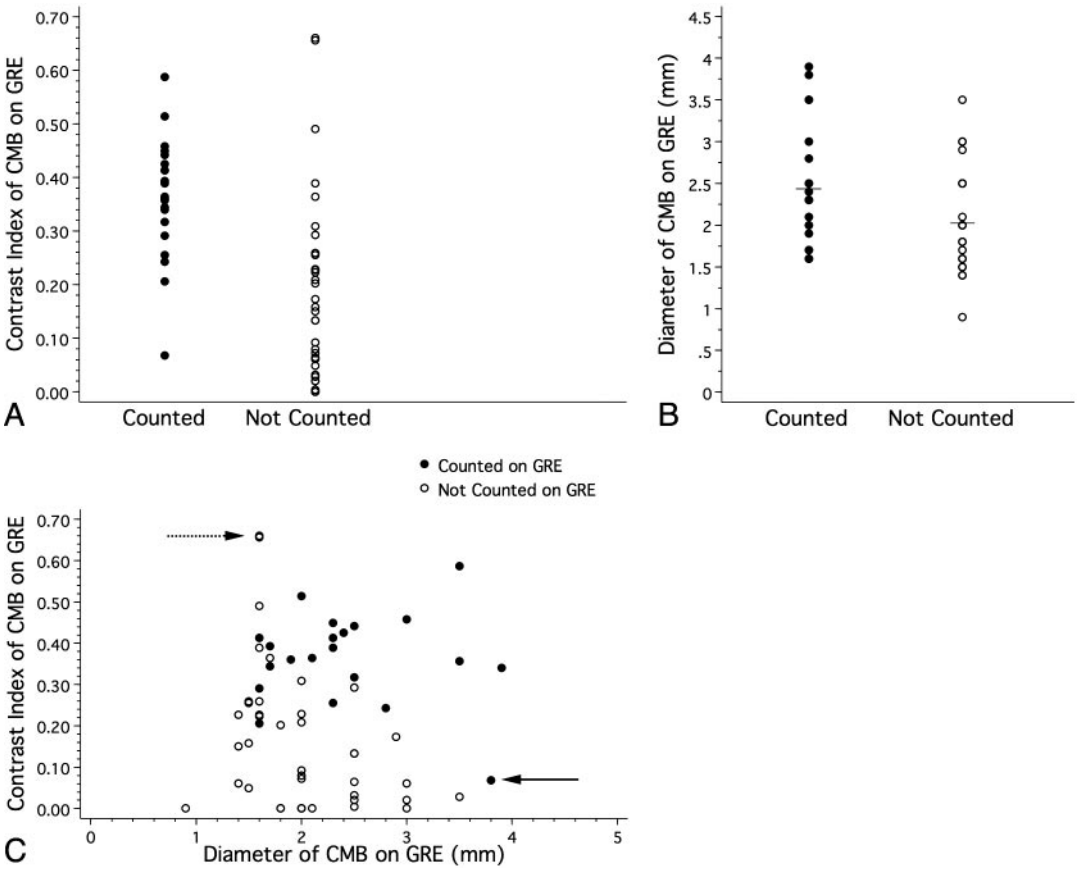

Fig 2. Detection of CMB as a function of lesion contrast and diameter. Scatterplots show CI (*A*), diameter (*B*), and a 2D plot of both parameters (*C*) of CMB prospectively identified (filled circles) or not prospectively identified (empty circles) by a blinded rater on clinical GRE MR images. *C,* The CMB in the lower right corner (*solid arrow*) were identified on GRE alone despite its lower CI, most likely because of its relatively large diameter. Conversely, the low-diameter CMB in the upper left corner of the figure (*dashed arrow*) were missed on GRE despite their relatively high CI. All measurements of CI and diameter were performed on the GRE images.

Previous reports have characterized the use of various SWI and high-resolution MR imaging techniques for diagnostic applications, such as venography,[28] brain tumors,[29] head trauma,[30] and vascular malformations.[31,32] Recent studies focusing on microbleed detection have also indicated increased sensitivity.[33,34] The Rotterdam Scan Study, by using a technique based on increased spatial resolution and prolonged TE without incorporation of phase information, demonstrated improved CMB detection relative to conventional GRE in a subset of 200 population-based subjects (prevalence of CMB, 35.5% versus 21.0%, $P < .001$) with no change in overall spatial distribution.[20] Another analysis of a single individual with hypertensive hemorrhage found that longer TEs resulted in an increased number and mean diameter of detected CMB.[35] Studies comparing 3T with 1.5T GRE MR imaging in brain trauma[21] and healthy aging have also demonstrated improved CMB detection.[22]

A specific strength of our study is its measurement of imaging characteristics of individual identified CMB across multiple scan types. There are also notable limitations. Although measurement of lesion contrast is relatively straightforward, lesion diameter is more difficult to measure with precision and required an indirect calculation. The imaging protocols developed and validated on our MR imaging systems include some differences in in-plane resolution and intersection gap (Table 1) that could have contributed to the observed effects on CMB CI and diameter, though such effects are expected to be small. For practical reasons, we could not study every possible permutation of sequence, resolution, and field strength and instead chose to focus on the 6 combinations shown in Table 1. The comparison of CMB counts shown in Table 3 involved 2 variations in MR imaging technique (SWI versus GRE and thin-versus-thick sections), each of which likely contributed to differences in CMB detection. Finally, the patients who participated in the present study were not (or only minimally) cognitively impaired, so it is not yet clear whether the scanning time of thin-section SWI (approximately 11 minutes) will be tolerable for patients with cognitive impairment, though our preliminary experience in such a population has been positive.

Recent studies have found CMB to be relatively common, not only in association with cerebrovascular disease, but also accompanying Alzheimer disease and normal aging.[5,6,13,14] Together with results from the Rotterdam Scan cohort,[6] our data suggest that implementation of more sensitive MR imaging techniques is likely to raise the estimated prevalence of CMB even further. Future studies will therefore be needed to define the clinical impact of these increasingly detectable lesions on questions such as risk of future hemorrhagic stroke,[12,16] whether a patient can be safely anticoagulated,[36] and risk of cognitive decline.[16,18]

Conclusions

SWI methods, smaller section thickness, and higher magnetic fields are each associated with significantly increased CMB contrast. In the case of thin-section SWI, increases in CI and lesion diameter are also associated with much higher rates of CMB detection. New imaging techniques are, therefore, very likely to increase the measured prevalence of CMB in the population.

Acknowledgments

The authors thank Dr. E. Mark Haacke for helpful discussions.

References

1. Jeerakathil T, Wolf PA, Beiser A, et al. **Cerebral microbleeds: prevalence and associations with cardiovascular risk factors in the Framingham Study.** *Stroke* 2004;35:1831–35. Epub 2004 May 20
2. Koennecke HC. **Cerebral microbleeds on MRI: prevalence, associations, and potential clinical implications.** *Neurology* 2006;66:165–71
3. Viswanathan A, Chabriat H. **Cerebral microhemorrhage.** *Stroke* 2006;37: 550–55
4. Cordonnier C, Al-Shahi Salman R, Wardlaw J. **Spontaneous brain microbleeds: systematic review, subgroup analyses and standards for study design and reporting.** *Brain* 2007;130:1988–2003
5. Sveinbjornsdottir S, Sigurdsson S, Aspelund T, et al. **Cerebral microbleeds in the population based AGES Reykjavik Study: prevalence and location.** *J Neurol Neurosurg Psychiatry* 2008;7:1002–06. Epub 2008 Feb 12
6. Vernooij MW, van der Lugt A, Ikram MA, et al. **Prevalence and risk factors of cerebral microbleeds: the Rotterdam Scan Study.** *Neurology* 2008;70:1208–14
7. Fazekas F, Kleinert R, Roob G, et al. **Histopathologic analysis of foci of signal loss on gradient-echo T2*-weighted MR images in patients with spontaneous intracerebral hemorrhage: evidence of microangiopathy-related microbleeds.** *AJNR Am J Neuroradiol* 1999;20:637–42
8. Tatsumi S, Shinohara M, Yamamoto T. **Direct comparison of histology of microbleeds with postmortem MR images: a case report.** *Cerebrovasc Dis* 2008;26:142–46
9. Greenberg SM, O'Donnell HC, Schaefer PW, et al. **MRI detection of new hemorrhages: potential marker of progression in cerebral amyloid angiopathy.** *Neurology* 1999;53:1135–38
10. Imaizumi T, Horita Y, Chiba M, et al. **Dot-like hemosiderin spots on gradient echo T2*-weighted magnetic resonance imaging are associated with past history of small vessel disease in patients with intracerebral hemorrhage.** *J Neuroimaging* 2004;14:251–57
11. Lee SH, Kwon SJ, Kim KS, et al. **Cerebral microbleeds in patients with hypertensive stroke: topographical distribution in the supratentorial area.** *J Neurol* 2004;251:1183–89
12. Soo YO, Yang SR, Lam WW, et al. **Risk versus benefit of anti-thrombotic therapy in ischaemic stroke patients with microbleeds.** *J Neurology* 2008. In press.
13. Atri A, Locascio JJ, Lin JM, et al. **Prevalence and effects of lobar microhemorrhages in early-stage dementia.** *Neurodegen Dis* 2005;2:305–12
14. Cordonnier C, van der Flier WM, Sluimer JD, et al. **Prevalence and severity of microbleeds in a memory clinic setting.** *Neurology* 2006;66:1356–60
15. Dichgans M, Holtmannspotter M, Herzog J, et al. **Cerebral microbleeds in CADASIL: a gradient-echo magnetic resonance imaging and autopsy study.** *Stroke* 2002;33:67–71
16. Greenberg SM, Eng JA, Ning M, et al. **Hemorrhage burden predicts recurrent intracerebral hemorrhage after lobar hemorrhage.** *Stroke* 2004;35:1415–20
17. Lee SH, Bae HJ, Kwon SJ, et al. **Cerebral microbleeds are regionally associated with intracerebral hemorrhage.** *Neurology* 2004;62:72–76
18. Werring DJ, Frazer DW, Coward LJ, et al. **Cognitive dysfunction in patients with cerebral microbleeds on T2*-weighted gradient-echo MRI.** *Brain* 2004;127:2265–75
19. Haacke EM, Xu Y, Cheng YC, et al. **Susceptibility-weighted imaging (SWI).** *Magn Reson Med* 2004;52:612–18
20. Vernooij MW, Ikram MA, Wielopolski PA, et al. **Cerebral microbleeds: accelerated 3D T2*-weighted GRE MR imaging versus conventional 2D T2*-weighted GRE MR imaging for detection.** *Radiology* 2008;248:272–77
21. Scheid R, Ott DV, Roth H, et al. **Comparative magnetic resonance imaging at 1.5 and 3 Tesla for the evaluation of traumatic microbleeds.** *J Neurotrauma* 2007;24:1811–16
22. Stehling C, Wersching H, Kloska SP, et al. **Detection of asymptomatic cerebral microbleeds: a comparative study at 1.5 and 3.0 T.** *Acad Radiol* 2008; 15:895–900
23. Chen YW, Gurol ME, Rosand J, et al. **Progression of white matter lesions and hemorrhages in cerebral amyloid angiopathy.** *Neurology* 2006;67:83–87
24. O'Donnell HC, Rosand J, Knudsen KA, et al. **Apolipoprotein E genotype and the risk of recurrent lobar intracerebral hemorrhage.** *N Engl J Med* 2000; 342:240–45
25. Knudsen KA, Rosand J, Karluk D, et al. **Clinical diagnosis of cerebral amyloid angiopathy: validation of the Boston criteria.** *Neurology* 2001;56:537–39
26. Sehgal V, Delproposto Z, Haacke EM, et al. **Clinical applications of neuroimaging with susceptibility-weighted imaging.** *J Magn Reson Imaging* 2005; 22:439–50
27. Cohen J. *Statistical Power Analysis for the Behavioral Sciences.* 2nd ed. Hillsdale, NJ: Lawrence Earlbaum Associates, 1988
28. Reichenbach JR, Venkatesan R, Schillinger DJ, et al. **Small vessels in the human brain: MR venography with deoxyhemoglobin as an intrinsic contrast agent.** *Radiology* 1997;204:272–77
29. Pinker K, Noebauer-Huhmann IM, Stavrou I, et al. **High-resolution contrast-enhanced, susceptibility-weighted MR imaging at 3T in patients with brain tumors: correlation with positron-emission tomography and histopathologic findings.** *AJNR Am J Neuroradiol* 2007;28:1280–86
30. Ashwal S, Babikian T, Gardner-Nichols J, et al. **Susceptibility-weighted imaging and proton magnetic resonance spectroscopy in assessment of outcome after pediatric traumatic brain injury.** *Arch Phys Med Rehabil* 2006;87:S50–58
31. Yoshida Y, Terae S, Kudo K, et al. **Capillary telangiectasia of the brain stem diagnosed by susceptibility-weighted imaging.** *J Comput Assist Tomogr* 2006;30:980–82
32. de Souza JM, Domingues RC, Cruz LC Jr, et al. **Susceptibility-weighted imaging for the evaluation of patients with familial cerebral cavernous malformations: a comparison with T2-weighted fast spin-echo and gradient-echo sequences.** *AJNR Am J Neuroradiol* 2008;29:154–58
33. Akter M, Hirai T, Hiai Y, et al. **Detection of hemorrhagic hypointense foci in the brain on susceptibility-weighted imaging: clinical and phantom studies.** *Acad Radiol* 2007;14:1011–19
34. Haacke EM, DelProposto ZS, Chaturvedi S, et al. **Imaging cerebral amyloid angiopathy with susceptibility-weighted imaging.** *AJNR Am J Neuroradiol* 2007;28:316–17
35. Tatsumi S, Ayaki T, Shinohara M, et al. **Type of gradient-recalled echo sequence results in size and number change of cerebral microbleeds.** *AJNR Am J Neuroradiol* 2008;29:e13
36. Eckman MH, Rosand J, Knudsen KA, et al. **Can patients be anticoagulated after intracerebral hemorrhage? A decision analysis.** *Stroke* 2003;34:1710–16